



ISSN (PRINT) : 2320 -1967
ISSN (ONLINE) : 2320 -1975



ORIGINAL ARTICLE

CHEMXPRESS 9(2), 192-205, (2016)

Vibrational analysis of the tautomers of the α -adrenergic agonist clonidine agent and their protonated species

Elida Romano, Silvia A. Brandán*

Cátedra de Química General, Facultad de Bioquímica, Química y Farmacia, Universidad Nacional de Tucumán, Ayacucho 471, 4000, San Miguel de Tucumán, Tucumán, (R. ARGENTINA)

E-mail: sbrandan@fbqf.unt.edu.ar

Received : 25th April, 2015 ; Revised : 15th September, 2015 ; Accepted : 20th September, 2015

Abstract : In the present work, a theoretical study on the structural and vibrational properties of three tautomers of the α -adrenergic agonist clonidine agent and their protonated species was reported by using the hybrid B3LYP method together with the 6-31G* and 6-311++G** basis sets. The inter-conversion between the three tautomers of clonidine and the reaction paths connecting these three structures with the corresponding transition states were studied by using the Synchronous Transit-Guided Quasi-Newton (STQN) method and those two levels of theory. The Natural Bond Orbital (NBO) and Atoms in Molecules theory (AIM) calculations were employed in order to evaluate their atomic charges, bond orders, stabilization energies and topological properties. The analysis of the frontier orbitals suggest that the pres-

ence of two Cl atoms in the phenyl rings is essential for increase the reactivity of a hydrochloride species. Moreover, the N-H group between the two phenyl and imidazoline rings increase the reactivity of clonidine hydrochloride, as compared with tolazoline hydrochloride. The study of the frontier orbitals predicted that the protonated form of clonidine is the less reactive in the gas phase. The tentative vibrational assignments for the four studied species were reported together with the force constants which were compared with those obtained for similar antihypertensive agents.

© Global Scientific Inc.

Keywords : Clonidine; Vibrational spectra; Molecular structure; Force field; DFT calculations.

INTRODUCTION

Our investigation group is centred in the study of heterocyclic compounds of pharmacological and medicinal interest, such as the isothiazole, benzothiazole, cyanopyridine, thiadiazole, fluoromethylated-pyrrol, nucleoside and quinolin

derivatives because they present a wide range of biological properties^[1-7]. For instance, the 2-(2-benzofuranyl)-2-imidazoline and tolazoline hydrochloride derivatives^[8,9] that contain furan and/or benzyl and imidazoline rings in its structures are antihypertensive agents, where the separation between two of their rings is an important requirements for

the interaction of these imidazolines with the α -adrenoceptors sites^[10]. In many cases, the incorporation of halogen atoms in their rings improves notably their pharmacological properties due to that change the structure-activity relationships. Then, the knowledge of this parameter together with the structural properties is useful and necessary to understand the mechanisms of interaction of the drug with the receptors sites, modes of action and behaviors in the different media. In this opportunity, we have studied the three tautomers and their protonated species of the antihypertensive 2-[2,6-dichlorophenylimino] imidazolidine agent, named clonidine that act as an agonist drug on the α -adrenoceptors sites^[11-13]. In recent times, a theoretical study on some antihypertensive agents, including clonidine were reported by Remko et al.^[14] but their atomic charges, stabilization energies, molecular electrostatic potentials, reactivity sites and vibrational analysis, so far, remain unknown. In a recent paper, we have studied clonidine hydrochloride whose structure is different from the neutral clonidine species because the incorporation of two additional H and Cl atoms in the structure of clonidine produces notable changes in their properties (*Romano et al. Submitted*). In this work, we have studied the structures and vibrational properties of the tautomers of neutral clonidine and their protonated species, in agreement with the experimental structure determined for the antihypertensive tolazoline hydrochloride^[10] and, as suggested for this species by Contreras et al^[9]. Then, the vibrational analyses for the tautomers and their protonated form were performed using the experimental available IR and Raman spectra of clonidine hydrochloride (*Romano et al. Submitted*) and DFT calculations in gas phase. Their force fields were computed at the same levels of theory by using the Scaled Quantum Mechanics Force Field (SQMFF) procedure^[15], the internal coordinates and the Molvib program^[16]. Hence, the complete assignments for these new species of clonidine were performed from the corresponding force fields using the two levels of approximation. Here, the inter-conversion between the three tautomers of clonidine and the reaction paths connecting these three structures with the correspond-

ing transition states found were for first time reported together with their calculated molecular force fields by using the B3LYP/6-31G* and B3LYP/6-311++G** combinations^[17,18]. Further natural bond orbital (NBO)^[19,20] and Atoms in Molecules (AIM)^[21,22] calculations were employed to study the atomic charges, molecular electrostatic potentials, stabilization energies and topological properties of all the species of clonidine in gas phase at the same levels of theory. In these species, as in clonidine hydrochloride and their dimer (*Romano et al. Submitted*), the reactivities were predicted using the frontier orbitals^[23,24]. Thus, different reaction sites are evidenced in the tautomers of clonidine and their protonated species, as compared with clonidine hydrochloride and their dimer suggesting that all these agonist species could interact with the α -adrenoceptors of diverse manners.

COMPUTATIONAL DETAILS

The *GaussView* program^[25] was used to model the initial structures of the tautomers and the protonated species of clonidine which were later optimized in gas phase using the hybrid B3LYP method^[17,18] and the 6-31G* and 6-311++G** basis sets with the Gaussian 09 program^[26]. The structures of the three tautomers of clonidine are those proposed by Remko et al.^[14], named IA, IB and II, while the protonated form was designed as (P). Figure 1 show these four optimized structures together with the atom's numberings. The inter-conversion between the three tautomers of clonidine and the reaction paths connecting these three structures were also investigated together with the two transition states expected. Here, the Synchronous Transit-Guided Quasi-Newton (STQN) method implemented by Schlegel et al.^[27] was used to search these two transition structures by using the Gaussian program^[26]. The atomic charges, bond orders and stabilization energies were calculated by means the NBO calculations^[19] with the NBO 3.1^[20] program while the topological properties were computed with the AIM2000 program^[22]. The force fields using those two levels approximation and the SQMFF procedure^[15] were computed with the Molvib program^[16]. The natural internal

ORIGINAL ARTICLE

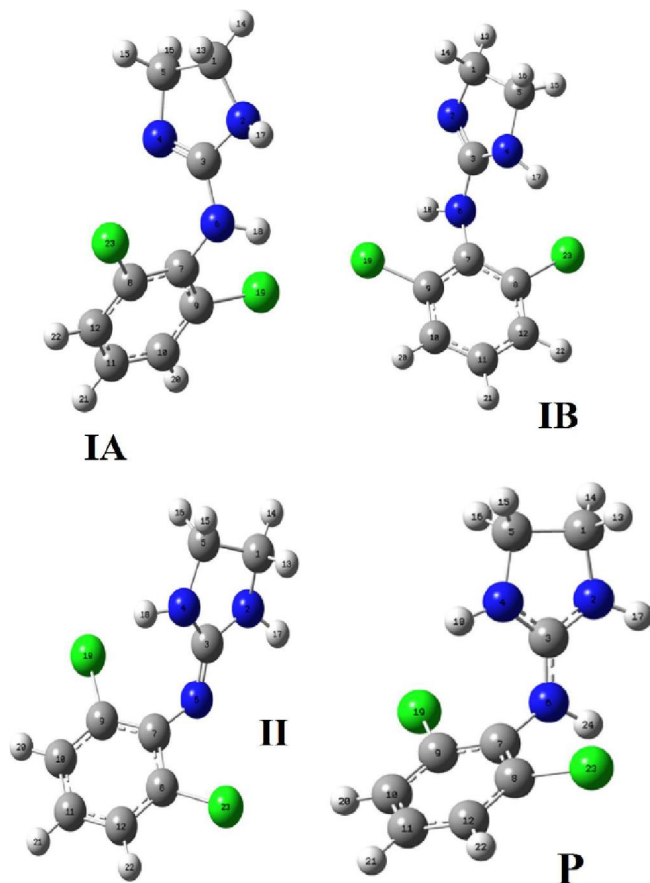


Figure 1 : Molecular structures of the three tautomers of clonidine and their protonated form together with the atoms numbering

coordinates for the tautomers of clonidine and their protonated species were not presented here because they are similar to those reported in the literature^[8,9]. The force fields and the potential energy distributions (PED) were employed to perform the complete assignments of the four species using the available vibrational spectra (*Romano et al. Submitted*). Furthermore, the force constants for the tautomers of clonidine and their protonated species were reported and compared with those calculated for clonidine hydrochloride (*Romano et al. Submitted*). Bands

attributed to the stable tautomers of clonidine were also observed in the vibrational spectra. The following reactivity order using the 6-31G* basis set was found when these species are compared with clonidine hydrochloride and with tolazoline hydrochloride (CIT) and their protonated (PT) species: $H > CIT > IB > PT > IA > II > P$ while the order change using the 6-311++G** basis set at: $H > CIT > IB > IA > PT > II > P$. Thus, the protonated species of clonidine is the less reactive species in gas phase using both levels of theory.

RESULTS AND DISCUSSION

Structures optimization

In TABLE S1 (Supporting Material) are presented the total and relative energies, and the dipole moment values for the three tautomers of clonidine by using both methods compared with the corresponding values for the protonated species. The complete analyses for the three tautomers of clonidine show clearly higher stability of the tautomeric II form using both basis sets, in accordance with their higher dipole moment values. Moreover, the inter-conversion between the three tautomers in the gas phase at the same theory levels and the relative energies among them can be seen in TABLE 1 while the reaction paths connecting these three structures and the two transition states found are given in Figure S1 (Supporting Material). Byre et al.^[28] have reported for clonidine hydrochloride that a strong barrier of energy impedes the rotation of the two torsion angles at the same time. In this case, the high dipole moment values for the tautomeric II form with both basis sets could in part explain their experimental stability, as was observed in other compounds^[29,30]. TABLE 2 summarize the calculated geometrical

TABLE 1 : B3LYP/6-31G* total energies (E) and relative energies (ΔE), and dipole moment (μ) for the tautomers of clonidine and the transition states connecting the minima in gas phase

Structure	E Hartree/molecule	ΔE kcal/mol	μ Debye
II	-1433.0210	0.00	3.77
QST1	-1432.7651	160.58	2.70
IB	-1433.0083	7.97	3.58
QST2	-1432.7721	156.19	2.36
IA	-1433.0084	7.90	1.37

TABLE 2 : Comparison of calculated geometrical parameters for the tautomers of clonidine and their protonated species with the experimental values corresponding to clonidine hydrochloride

Parameter	Exp. ^b	B3LYP ^a							
		IA		IB		II		Protonated	
		6-31G*	6-311++G**	6-31G*	6-311++G**	6-31G*	6-311++G**	6-31G*	6-311++G**
Bond lengths (Å)									
C(1)-N(2)	1.447	1.476	1.477	1.469	1.469	1.460	1.461	1.476	1.477
C(1)-C(5)	1.533	1.560	1.557	1.553	1.550	1.539	1.538	1.545	1.544
N(2)-C(3)	1.321	1.403	1.401	1.283	1.281	1.382	1.381	1.343	1.341
C(3)-N(4)	1.322	1.278	1.274	1.397	1.395	1.388	1.385	1.339	1.336
N(4)-C(5)	1.450	1.469	1.470	1.474	1.476	1.464	1.465	1.475	1.476
C(3)-N(6)	1.328	1.398	1.394	1.396	1.392	1.285	1.282	1.337	1.334
N(6)-C(7)	1.418	1.408	1.407	1.407	1.405	1.386	1.385	1.430	1.430
C(7)-C(8)	1.392	1.408	1.405	1.409	1.407	1.415	1.412	1.406	1.404
C(7)-C(9)	1.391	1.407	1.404	1.411	1.409	1.414	1.412	1.406	1.404
C(9)-C(10)	1.382	1.392	1.389	1.392	1.389	1.393	1.390	1.393	1.391
C(10)-C(11)	1.377	1.392	1.390	1.393	1.391	1.393	1.391	1.394	1.392
C(11)-C(12)	1.371	1.393	1.391	1.393	1.390	1.394	1.392	1.395	1.392
C(8)-C(12)	1.385	1.393	1.390	1.393	1.390	1.391	1.388	1.393	1.390
C(8)-Cl(23)	1.724	1.750	1.750	1.759	1.758	1.757	1.756	1.745	1.745
C(9)-Cl(19)	1.733	1.762	1.761	1.756	1.755	1.766	1.764	1.749	1.747
RMSD		0.035	0.034	0.033	0.032	0.032	0.031	0.018	0.017
Bond angles (°)									
C(1)-N(2)-C(3)	111.5	104.9	105.1	105.7	106.1	110.0	110.1	110,3	110,4
N(2)-C(3)-N(4)	111.8	118.3	118.0	117.8	117.4	107.5	107.5	110,7	110,7
N(2)-C(1)-C(5)	102.6	101.7	101.6	105.8	105.4	100.7	100.8	101,5	101,5
C(3)-N(4)-C(5)	110.6	105.9	106.3	104.7	104.8	109.6	109.8	110,4	110,6
C(1)-C(5)-N(4)	103.5	106.3	106.1	101.2	101.0	101.0	101.0	101,6	101,6
N(2)-C(3)-N(6)	123.1	115.6	116.1	121.2	121.6	122.5	122.8	124,4	124,5
C(3)-N(6)-C(7)	123.0	121.0	121.0	125.1	125.4	122.1	122.0	124,2	124,0
N(6)-C(3)-N(4)	125.2	126.0	125.9	120.9	120.9	129.9	129.6	124,9	124,8
N(6)-C(7)-C(8)	121.3	121.8	121.7	122.4	122.4	120.7	121.0	120,0	120,2
N(6)-C(7)-C(9)	121.4	121.5	121.5	121.3	121.2	123.9	123.5	121,1	120,9
C(8)-C(7)-C(9)	117.3	116.6	116.7	116.1	116.2	115.1	115.2	118,8	118,8
C(7)-C(9)-C(10)	121.5	122.5	122.4	122.5	122.4	123.0	122.9	120,7	120,7
C(9)-C(10)-C(11)	119.8	119.2	119.2	119.4	119.4	119.5	119.5	119,3	119,3
C(10)-C(11)-(12)	120.2	120.1	120.2	120.1	120.1	119.8	119.8	121,1	121,1
C(11)-C(12)-C(8)	119.8	119.9	119.8	119.6	119.6	119.7	119.7	119,3	119,3
C(12)-C(8)-C(7)	121.4	121.6	121.6	122.2	122.2	122.8	122.8	120,8	120,8
C(7)-C(9)-Cl(19)	120.0	119.1	119.1	119.0	119.0	119.0	119.0	119,9	119,8
C(10)-C(9)-Cl(19)	118.5	118.4	118.5	118.5	118.6	118.0	118.1	119,4	119,4
C(7)-C(8)-Cl(23)	119.9	120.1	120.0	119.9	119.8	118.6	118.6	119,5	119,6
C(12)-C(8)-Cl(23)	119.7	118.2	118.3	117.8	117.9	118.5	118.6	119,7	119,6
RMSD		3.02	2.86	2.79	2.68	1.94	1.85	0.95	0.93
Dihedral angles (°)									
N(2)-C(3)-N(6)-C(7)	178.1	179.6	179.8	159.7	163.2	176.9	176.3	179.3	178.5
N(4)-C(3)-N(6)-C(7)	0	-1.1	-1.7	-17.5	-13.7	-5.2	-5.7	-0.2	-1.2
C(3)-N(6)-C(7)-C(8)	-76.5	-69.8	-70.2	-77.4	-75.9	-74	-76	-78.3	-81.9
C(3)-N(6)-C(7)-C(9)	105.2	114.2	113.1	106.9	108.1	112.2	110.1	104.6	100.4
RMSD		5.69	5.19	12.73	10.23	4.58	3.87	1.13	3.67

^aThis work, ^b Ref [28]

ORIGINAL ARTICLE

parameters for the three tautomers of clonidine and their protonated form compared with the experimental values determined by Byre et al.^[28] for clonidine hydrochloride by means of the root mean of square deviation (RMSD) values. In the tautomer II and P, the bond N(2)-C(3) and C(3)-N(4) lengths belong to the imidazoline ring are chemically equivalent, as in the experimental structure, because both N atoms are protonated. This observation is very important taking into account that in the agonist compounds, as clonidine, the positive charge is evenly distributed in the N-C-N region of the imidazole ring, as reported for tolazoline hydrochloride^[10]. A contrary result it is observed in the tautomers IA and IB. Thus, a double bonds character are observed in the N(2)-C(3) bond of IB and in the C(3)-N(4) bond of IA. Moreover, the bond C(3)-N(6) length in the tautomer II is different from that corresponding to the P species due to their double partial character bond. The calculated bond C(3)-N(6)-C(7) angle value differ notably in all these species, as observed in TABLE 2. The analysis of the geometrical parameters using the RMSD values show a very good correlation for all the structures of clonidine but particularly, the protonated form present the better correlation in the bond lengths and angles and in the dihedral angles, as observed in TABLE 2. The lower RMSD values observed for P and the tautomer II suggest clearly the presence of these forms in the solid state, as observed in TABLE 2. Hence, these B3LYP/6-31G* and B3LYP/6-311++G** structures can be a reliable starting point for the determination of their frequencies and force fields.

NPA, MEP and Wiberg index studies

For the three tautomers of clonidine and their P species, NBO calculations^[19,20] were employed to study the natural population atomic charges (NPA) and the bond order expressed as Wiberg indexes using both approximation levels because the charge distributions in these species could explain the form of interaction between a agonist drug, as clonidine with their α -adrenergic receptor site, as suggested by Ghose and Dattagupta^[10]. Here, the presence of two Cl atoms in the benzyl rings probably has influence on the stabilities of the tautomers of clonidine

and their P species. Hence, the NPA charges for these species in gas phase at different theory levels can be seen in TABLE S2. The complete analysis for the four structures show that the most positive NPA values are observed on the C3 atoms belonging to the imidazole rings while the most negative values are observed on the N atoms of all the species. Analyzing the most positive NPA values on the H atoms, we observed that the P form present the higher values using both basis sets, in relation to the other ones. Here, probably the proximity between the H17 and H18 atoms together with their NPA charges can in part explain the lower stability of the IA structure of clonidine, in relation to the tautomers II and IB.

For the four structures of clonidine we have also studied the molecular electrostatic potential (MEP) surface mapped at B3LYP/6-31G* level in order to find the possible reaction sites of these agonist species that interaction with potential biological nucleophiles or electrophiles sites. The surface mapped for the tautomer II of clonidine and their protonated form were performed using the Gaussian program^[26] and the graphics are given in Figures S2 and S3, respectively. We observed that the difference between the surfaces mapped are notable, thus, for the neutral tautomer II of clonidine, Figure S2 shows a strong red colour on the N6 atom which is not protonated suggesting that this region act as an electrophilic site, acceptor of H bonds and, for this reason, reacting with potential biological nucleophiles while the N2-H17 bond exhibit the coloration blue typical of the nucleophilic sites, donor of H bonds reacting with potential biological electrophiles. Obviously, the capability of hydrogen bond formation can be with share of nitrogen atoms of the imidazoline ring or through hydrogen atom of -NH moieties.

In TABLE S3 are summarized the bond orders, expressed by Wiberg's index for the tautomers of clonidine and the P form. It is notable the strong dependence of the size of the basis sets on the bond order values, hence, the values slightly increase when increase the size of the basis set. Note that the highest bond order values are observed in the C8 and C9 atoms belong to the phenyl rings and linked to the Cl atoms while the lowest values are calculated for the C1 and C5 atoms belonging to the

imidazoline rings. On the other hand, similar values are observed in the bond orders for the N2 and N4 atoms of the II tautomer and for P, as expected because both atoms show clearly that are chemically equivalent due to that they are protonated, as observed in the structural parameters.

NBO analysis

The second order perturbation energies that involve the most important delocalization are important parameters to evaluate the stabilities of different species using NBO calculations^[19,20]. For this reason, the three tautomers of clonidine and their P form were also analyzed by using the stabilization energy values which are presented in TABLE S4. In general, there are four delocalization energies similar for all the species whose values do not shown a defined tendency, which are the $\Delta ET_{\sigma \rightarrow \sigma^*}$, $\Delta ET_{\pi \rightarrow \pi^*}$, $\Delta ET_{LP \rightarrow \pi^*}$ and $\Delta ET_{\pi^* \rightarrow \pi^*}$ charge transfers. However, the P species show the $\Delta ET_{LP \rightarrow LP^*C3}$ charge transfer from the three N atoms to the C atoms attached to them, which also contributes to its high stability. For the tautomers of clonidine, the contributions to the ΔET_{Total} stabilization energies follow the tendency: II (3027.46 kJ/mol) > IA (2716.45 kJ/mol) > IB (2539.85 kJ/mol) by using the 6-31G* basis set while a contrary result is observed when the 6-311++G** basis set is employed (IA > IB > II). Hence, we observed that the stabilization energy values are strongly dependent of the size of the basis set. This NBO study for the three tautomers of clonidine has revealed only two delocalizations $\Delta ET_{\sigma \rightarrow \sigma^*}$ attributed to the imidazole ring in the IA and IB structures absent in the structure II. However, the total energy values ΔE_{Total} confirm the greater stability of the tautomer II in relation to the tautomers IA and IB. This study support clearly the high stabilities of the tautomer II and their protonated form.

AIM study

The presence of intra-molecular interactions that confer stability to the tautomers of clonidine and their protonated form are of interest taking into account that these are species with agonist activity^[10]. Thus, we have investigated in the four structures of clonidine by using the Bader's theory and the AIM2000 program^[21,22] the charge electron density,

$\rho(r)$ and the Laplacian values, $\nabla^2\rho(r)$ in the bond critical points (BCPs) and ring critical points (RCPs). These topological properties for the phenyl and imidazoline rings in the RCPs are given in TABLE S5 while the parameters corresponding to the BCPs and new RCPs are presented in TABLE S6. We observed that the $\rho(r)$ and $\nabla^2\rho(r)$ values of the imidazoline rings are higher and slightly different from the properties corresponding to the phenyl rings which are practically the same because in those structures the rings do not change. These results show clearly the different character of both rings. For both tautomers IA and IB, we observed two new bond critical points (BCP), that involving the chlorine atom, and the formation of a new ring critical point, whose $\rho(r)$ and $\nabla^2\rho(r)$ values are lower than the other two rings. Here, the additional BCPs in IA and IB probably confer to these two forms high stabilities and, for this reason, these species could be present in the solid state.

Vibrational analysis

The optimized structures of the three tautomers and their protonated form present C_1 symmetries and 63 and 66 vibration normal modes, respectively where all the vibration modes have activity in both infrared and Raman spectra. Figures 2 and 3 show the experimental available IR and Raman spectra (Romano et al. Submitted) which were compared with the corresponding average theoretical spectra of the three tautomers and the protonated form of clonidine at the B3LYP/6-31G* level of theory. It is necessary to clarify that in both experimental spectra were observed bands attributed to the tautomers and to the P form of clonidine. The observed and calculated frequencies together with the assignments for all the tautomers and the protonated species are summarized in TABLE 3. The assignments were performed considering only the PED contributions $\geq 10\%$ by using the B3LYP/6-31G* method, the corresponding symmetry coordinates, scale factors reported at the same level of theory^[15] and taking into account the assignments of related molecules^[1-9,24,29,30]. From TABLES S7 to S10 are presented the assignments for all the tautomers and the protonated species together with the PED contributions based

ORIGINAL ARTICLE

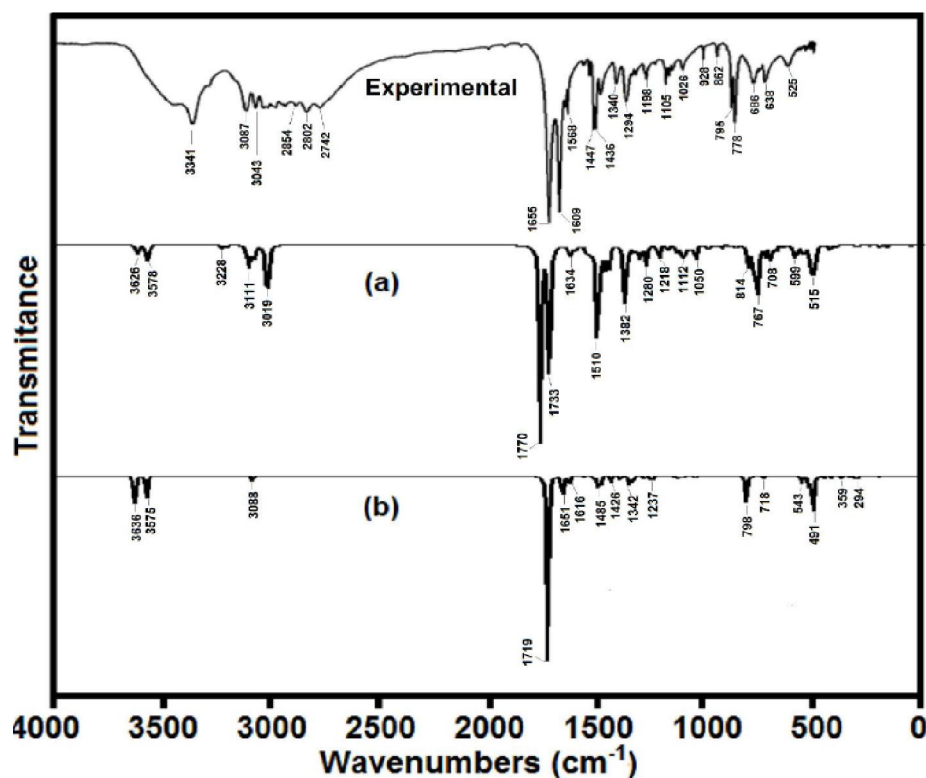


Figure 2 : Experimental available infrared spectrum (Romano et al. Submitted, 2015) compared with the corresponding average theoretical spectra of the three tautomers and the protonated form of clonidine at the B3LYP/6-31G* level of theory

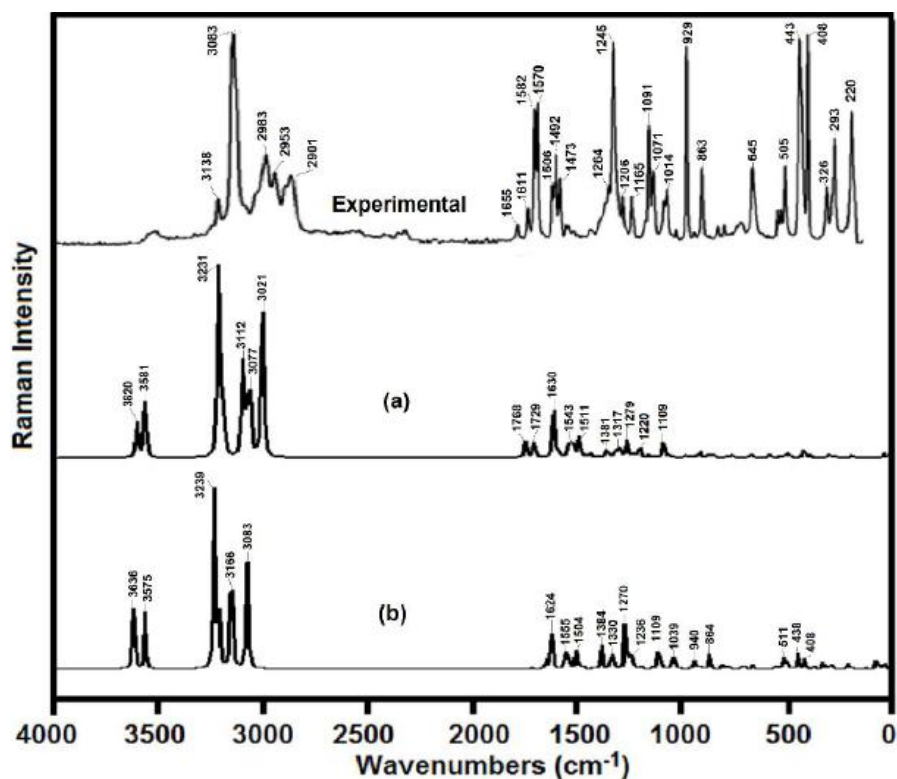


Figure 3 : Experimental available Raman spectrum (Romano et al. Submitted, 2015) compared with the corresponding average theoretical spectra of the three tautomers and the protonated form of clonidine at the B3LYP/6-31G* level of theory

TABLE 3 : Observed and calculated wavenumbers (cm⁻¹) and assignment for the tautomers of clonidine and their prototated form

Experimental ^a		IA		IB		II		Protonated	
IR	Raman	SQM ^b	Assignment ^a						
						3471	v (N2-H17)	3485	v (N4-H18)
						3465	v (N4-H18)	3479	v (N2-H17)
3427 m, br	3422 vw			3433	v (N2-H17)			3427	v (N6-H24)
	3411 vw	3411	v (N6-H18)						
3341 s	3346 w, br	3401	v (N2-H17)	3426	v (N6-H18)				
3135 sh	3138 m							3108	v(C-H) ip
	3093 sh	3099	v(C10-H20)	3100	v(C12-H22)	3095	v (C12-H22)	3105	v(C-H) op ₂
3087 s	3083 vs	3095	v(C12-H22)	3095	v(C10-H20)	3089	v(C10-H20)	3088	v(C-H) op ₁
3043 m	3050 m	3074	v(C11-H21)	3076	v(C11-H21)	3071	v (C11-H21)	3035	v _{as} (CH ₂)ip
3007 m	3005 sh							3026	v _{as} (CH ₂)op
2986 m	2983 s	2975	v _{as} CH ₂ (C1)	2977	v _{as} CH ₂ (C5)	2988	v _{as} CH ₂ (C5)		
2960 sh		2954	v _{as} CH ₂ (C5)	2957	v _{as} CH ₂ (C1)	2983	v _{as} CH ₂ (C1)	2960	v _s (CH ₂)op
2950 m	2953 m							2956	v _s (CH ₂)ip
2920 sh	2919 m	2916	v _s CH ₂ (C5)						
2906 m	2901 m	2910	v _s CH ₂ (C1)	2902	v _s CH ₂ (C1)	2905	v _s CH ₂ (C5)		
2872 sh				2895	v _s CH ₂ (C5)	2892	v _s CH ₂ (C1)		
2854 m	2822 vw								
2802 m	2811 vw								
2742 m	2792 vw								
1655 vs	1655 m	1683	v(C3-N4)	1660	v (C3-N2)	1700	v (C3-N6)	1651	v _{as} (CN ₃)
1609 s	1611 m							1590	v _{as} (CN ₃)
1581 m	1582 s	1582	v(C9-C10)	1580	v(C9-C10)				
1568 m	1570 s	1570	v(C10-C11)	1559	v(C11-C12)	1576	v(C=C)ip ₃	1570	v(C=C)ip ₃
	1542 sh					1546	v(C=C)ip ₂	1562	v(C=C)ip ₂
1506 w	1506 m	1508	v (C3-N6)						
1493 w	1492 m	1495	δCH ₂ (C1)	1489	δCH ₂ (C5)	1488	δ CH ₂ (C1)	1486	δ (CH ₂) ip
1485 w	1473 m	1486	δCH ₂ (C1)	1468	δCH ₂ (C1)	1485	δ CH ₂ (C5)	1472	δ (CH ₂) op
1466 w		1467	δCH ₂ (C5)	1452	v(C7-C9)				
1447 s	1446 m	1449	β(C12-H22)	1445	β(C12-H22)	1448	v(C=C)op ₁	1444	β(C12-H22)
1436 s	1436 w	1435	β(N2-H17)	1442	β(N4-H17)	1430	v(C=C)op ₃	1439	β(C10-H20)
1414 m	1416 w, br	1410	β(N6-H18)			1424	v(C3-N4)	1420	β (N6-H24)
	1395 w					1407	wg CH ₂ (C1)		
1385 sh	1380 w			1388	β(N6-H18)	1329	β(N2-H17)	1374	wg (CH ₂)op
1340 m	1342 w	1340	wg CH ₂ (C5)	1349	wg CH ₂ (C5)	1326	β(N4-H18)	1319	β(N4-H18) β(N2-H17)*
1294 m	1293 sh	1312	wg CH ₂ (C1)	1310	wg CH ₂ (C1)			1304	wg (CH ₂)ip
	1278 sh	1281	v(C7-C8)	1283	v (C3-N6)	1276	wg CH ₂ (C5)	1281	v(C=C)op ₁
1264 w	1264 m	1249	v(C8-C12); v(C7-C9)*	1269	v(C7-C8)	1257	v(C=C)op ₂	1267	v(C=C)op ₂
1246 w	1245 s	1231	ρ CH ₂ (C5)	1233	v(C8-C12)	1241	v(C7-N6)	1233	v(C7-N6)
1206 w	1206 m	1221	v (C3-N2)	1220	ρ CH ₂ (C1)			1211	ρ CH ₂ (C5)
1198 w						1196	ρ CH ₂ (C1)	1206	ρ CH ₂ (C1)
	1194 sh	1194	β (C10-H20)	1185	β(C10-H20)	1188	β(C-H) ip	1200	v(C=C)op ₃
	1165 m	1179	ρ CH ₂ (C1)	1176	ρ CH ₂ (C5)	1181	ρ CH ₂ (C5)		

ORIGINAL ARTICLE

Experimental ^a			IA	IB			II	Protonated	
IR	Raman	SQM ^b	Assignment ^a	SQM ^b	Assignment ^a	SQM ^b	Assignment ^a	SQM ^b	Assignment ^a
1155 vw	1157 sh	1149	β (C11-H21)	1148	β (C11-H21)	1144	β (C10-H20)	1160	β (C11-H21)
	1127 vw								
1111 sh									
1105 m	1105 w								
1091 w	1091 s	1078	βR_1 <i>benc.</i>	1078	βR_1 <i>benc.</i>	1078	β (C-H) <i>op</i>	1090	βR_1 <i>benc.</i>
1075 w	1071 m	1070	ν (C11-C12)	1070	ν (C10-C11)	1066	ν (C=C) <i>ip</i> ₁	1069	ν (C=C) <i>ip</i> ₁
1069 w		1051	ν (C5-N4)	1040	ν (C5-N4)	1062	ν (C5-N4)	1055	ν (C5-N4)
1026 w	1028 m	1037	ν (C1-N2)	1020	ν (C1-N2)	1022	τw CH ₂ (C1)	1021	τw CH ₂ (C5)
	1014 m					1019	ν (C1-N2)	1008	ν_s (CN ₃)
	987 vw	999	$\tau\omega$ CH ₂ (C5)	1002	τw CH ₂ (C5)			996	γ (C-H) <i>op</i> ₁
973 w	973 vw	975	βR_1 <i>imid.</i>	977	βR_1 <i>imid.*</i>	961	ν (C3-N2)		
928 w	929 s	957	γ (C11-H21)	962	γ (C11-H21)	946	γ (C11-H21)	912	γ (C-H) <i>op</i> ₂
	898v w	891	γ (C10-H20)	896	ν (C1-C5)	911	ν (C1-C5)	902	ν (C1-C5)
	877 vw	889	ν (C1-C5)	894	γ (C10-H20)	890	γ (C12-H22)		
862 w	863 m	862	ν (C7-N6)	860	ν (C7-N6)	868	τw CH ₂ (C5)	858	τw CH ₂ (C5) τw CH ₂ (C1)*
	840 vw	857	γ (C11-H21)			841	βR_1 <i>benc.</i> ; βR_1 <i>imid.*</i>		
	828 vw	832	ν (C5-N4)*						
812 sh				825	τw CH ₂ (C1)			834	τw CH ₂ (C1)
795 m	794 w	802	βR_2 <i>imid.</i>	794	γ (C7-N6)				
778 s	778 vw	771	γ (C12-H22)	773	γ (C12-H22)	773	τw <i>benc.</i>	778	ν (C-Cl) <i>op</i>
	766 w	759	βR_2 <i>benc.</i>	753	βR_2 <i>benc.</i>	763	γ (C10-H20)	759	βR_1 <i>imid.</i>
	747 vw	750	τw CH ₂ (C1)	744	γ (N4-H17)	753	ν (C-Cl) <i>op</i>		
	713 vw					718	γ C3-N6		
694 m	696 w, br	701	γ (C7-N6)	694	τR_1 <i>benc.</i>			700	γ C3-N6
686 m				671	βR_3 <i>benc.</i>	688	βR_3 <i>benc.</i>	686	βR_2 <i>imid.</i>
669 w		669	βR_3 <i>benc.</i>	666	γ C3-N6	672	βR_2 <i>imid.</i>	680	τR_1 <i>benc.</i>
638 w	645 m	638	γ C3-N6			633	τR_1 <i>benc.</i>	644	βR_3 <i>benc.</i>
618 sh	600 vw	612	γ N2-H17						
	587 vw			585	βR_2 <i>imid.</i>				
	578 vw					574	γ N2-H17		
532 w	537 w	544	τR_1 <i>benc.</i>	544	τR_3 <i>benc.</i>	539	β (C7-N6)	538	β (C7-N6)
525 w	522 w					516	γ (C8-Cl23)	527	γ (C-Cl) <i>op</i>
518 w		517	γ (C8-Cl23); γ (C9-Cl19)*	519	γ (C9-Cl19)	509	γ (C9-Cl19)	499	τR_3 <i>benc.</i>
501 w	505 m	508	γ N6-H18	512	γ (N6-H18)	499	γ (N4-H18)	489	γ (N4-H18)
486 w		493	β (C7-N6)	489	β (C7-N6)			485	γ (N2-H17) γ (N6-H24)
462 vw	443 s								
437 vw	437 sh								
421 w, br		413	ν (C9-Cl19)	421	ν (C9-Cl19)			425	ν (C-Cl) <i>ip</i>
406 w	408 vs					425	β (C3-N6)		

Experimental ^a			IA	IB		II		Protonated	
IR	Raman	SQM ^b	Assignment ^a	SQM ^b	Assignment ^a	SQM ^b	Assignment ^a	SQM ^b	Assignment ^a
402 vw		399	$\nu(\text{C8-C123})$	396	$\nu(\text{C8-C123})$	399	$\beta\text{R}_2 \text{ benc.}$	399	$\beta(\text{C8-C123})$
								356	$\gamma(\text{N2-H17})$ $\gamma(\text{N6-H24})$
	326 m	322	$\beta(\text{C9-C119})$	314	$\beta(\text{C3-N6})$	315	$\nu(\text{C-Cl})\text{ip}$	311	$\beta\text{R}_2 \text{ benc.}$
	303 sh			300	$\tau\text{W} \text{ benc.}$ $\beta(\text{C7-N6})^*$			289	$\beta(\text{C3-N6})$
	293 m	299	$\beta(\text{C8-C123})$			301	$\beta(\text{C9-C119})$ $\gamma(\text{C9-C119})$		
	268 vw	277	$\beta(\text{C3-N6})$	268	$\gamma(\text{C8-C123})$	279	$\gamma(\text{C8-C123});$ $\tau\text{R}_3 \text{ benc.}^*$	278	$\gamma(\text{C-Cl}) \text{ ip}$
	260 vw								
	220 s								
	210 sh	207	$\tau\text{R}_2 \text{ imid.}$	206	$\beta(\text{C8-C123})$	240	$\tau\text{R}_1 \text{ imid.}$		
		202	$\tau\text{R}_2 \text{ benc.}$	202	$\tau\text{R}_2 \text{ benc.}$	204	$\tau\text{R}_2 \text{ benc.}$	196	$\tau\text{R}_2 \text{ benc.}$
	186 vw	196	$\beta(\text{C9-C119}) \beta(\text{C8-C123})^*$	197	$\beta(\text{C9-C119})$	192	$\beta(\text{C8-C123})$	193	$\beta(\text{C9-C119})$
								177	$\tau\text{R}_2 \text{ imid.}$
	169 w, br			163	$\tau\text{R}_2 \text{ imid.}$	166	$\tau\text{R}_2 \text{ imid.}$	169	$\tau\text{R}_1 \text{ imid.}$
	126 vw	126	$\tau\text{R}_1 \text{ imid.}$	126	$\tau\text{R}_1 \text{ imid.}$				
	119 vw	111	$\delta(\text{C3N6C7})$						
	109 vw					109	$\delta(\text{C3N6C7})$	109	$\gamma \text{ C7-N6}$
						66	$\tau\text{W} \text{ imid.}$		
		62	$\tau\text{R}_3 \text{ benc.}$	61	$\delta(\text{C3N6C7})$			61	$\delta(\text{C3N6C7})$
		53	$\tau\text{W} \text{ imid.}$	52	$\tau\text{W} \text{ imid.}$	58	$\tau\text{R}_3 \text{ benc.}$	44	$\tau\text{W} \text{ imid.}$
		39	$\tau\text{W} \text{ benc.}$	30	$\tau\text{W} \text{ benc.}$	28	$\tau\text{W} \text{ benc.}$	22	$\tau\text{W} \text{ benc.}$

^aThis work; ^bFrom scaled quantum mechanics force field

on the 6-31G* basis set. The SQM force fields for these species can be obtained at request to the authors. Below we have discussed the assignments of some groups.

Band assignments

NH modes

The N-H stretching modes expected for these species are associated to the bands observed between 3427 and 3341 cm^{-1} in both spectra, as indicated in TABLE 3 while the group of bands of different intensities at 2854, 2802 and 2742 cm^{-1} are assigned to the NH stretching modes corresponding to the protonated nitrogen atoms of the imidazole rings belonging to the dimer of clonidine (*Romano et al. Submitted*). The bands in the 1436-1340 cm^{-1} region are assigned to the in-plane deformations modes while the corresponding out-of-plane deformations are associated to the shoulder in the IR at

618 cm^{-1} and to the intense band in the Raman spectrum at 505 cm^{-1} and a shoulder at 437 cm^{-1} , in agreement with similar compounds^[2,4-6,8,9].

CN modes

The bands that show different intensities at 1655 cm^{-1} , 1246 cm^{-1} and 862 cm^{-1} in IR and Raman spectra are assigned to the C-N stretching modes of all the species of clonidine, as indicated in TABLE 3. Moreover, the SQM calculations predicted for the group N-C-N of the P form, antisymmetric and symmetric stretching modes which are indicated as CN_3 in TABLE 3. Thus, the two antisymmetric stretching modes appear as strong bands in the IR at 1655 and 1609 cm^{-1} , which are associated to bands of medium intensity in the Raman spectrum at 1655 and 1611 cm^{-1} , respectively. The symmetric stretching of that group is only observed in the Raman spectrum at 1014 cm^{-1} , with medium intensity, as can be seen in TABLE 3. Here, the weak Raman band at

ORIGINAL ARTICLE

TABLE 4 : Comparison of scaled internal force constants for the tautomers, hydrochloride and protonated forms of clonidine using two levels of theory

B3LYP/6-31G*							
Description	Clonidine ^a					BFI ^b	T ^c
	IA	IB	II	H [#]	P		
$f(\nu N-H)$	6.44	6.53	6.67	5.21	6.54	6.53	6.68
$f(\nu N-C)$	5.92	5.92	6.16	6.11	6.16	4.75	4.48
$f(\nu C-H)_{imid}$	4.57	4.55	4.58	4.67	4.79	4.78	4.94
$f(\nu C-H)_{benc}$	5.23	5.24	5.22	5.26	5.28	5.17	5.17
$f(\nu C-Cl)$	3.28	3.27	3.21	3.32	3.29		
$f(\nu Cl-H)$				0.88			
$f(\nu C-C)_{imid}$	3.66	3.73	4.00	3.94	4.15	3.86	4.21
$f(\nu C-C)_{benc}$	6.53	6.49	6.42	6.58	6.53	6.58	6.50
$f(\beta_R)_{benc}$	0.22	0.22	0.22	0.22	0.22	0.35	0.22
$f(\beta_R)_{imid}$	0.33	0.33	0.34	0.33	0.33		0.34
$f(\gamma C-H)$	0.43	0.44	0.43	0.44	0.45		0.47

B3LYP/6-311++G**							
Description	Clonidine ^a					BFI ^b	T ^c
	IA	IB	II	H [#]	P		
$f(\nu N-H)$	6.50	6.57	6.70	5.33	6.66	6.57	6.66
$f(\nu N-C)$	5.79	5.78	6.03	5.99	6.04	4.63	4.38
$f(\nu C-H)_{imid}$	4.51	4.49	4.52	4.60	4.66	4.72	4.86
$f(\nu C-H)_{benc}$	5.16	5.16	5.15	5.18	5.18	5.10	5.09
$f(\nu C-Cl)$	3.24	3.24	3.18	3.28	3.40		
$f(\nu Cl-H)$				0.81			
$f(\nu C-C)_{imid}$	3.61	3.69	3.95	3.89	3.93	3.81	4.12
$f(\nu C-C)_{benc}$	6.40	6.36	6.29	6.46	6.36	6.50	6.02
$f(\beta_R)_{benc}$	0.22	0.22	0.22	0.22	0.22	0.35	0.22
$f(\beta_R)_{imid}$	0.33	0.33	0.33	0.33	0.33		0.34
$f(\gamma C-H)$	0.43	0.43	0.43	0.43	0.45		0.47

Units in $\text{mdyn } \text{\AA}^{-1}$ for stretching and $\text{mdyn } \text{\AA} \text{ rad}^{-2}$ for angle deformations, ν , stretching; β , deformation; γ , out plane deformation; benc., benzene; imid., imidazole; R, ring, ^aThis work, ^bFrom Ref [8] for 2-(-2-benzofuranyl)-2-imidazole, ^cFrom Ref [9] for the protonated species of tolazoline hydrochloride, [#]From Romano et al. Submitted

1127 cm^{-1} is clearly assigned to the CN stretching modes of the dimer (Romano et al. Submitted) whereas the CNC deformation corresponding to the dimer is assigned to the strong band at 443 cm^{-1} .

CH modes

The bands between 3087 and 3043 cm^{-1} in the IR spectrum and between 3093 and 3050 cm^{-1} in the Raman spectrum are clearly assigned to the C-H stretching modes, in accordance to similar compounds^[1-9]. The corresponding in-plane deformations modes of these groups are easily assigned to the IR bands at 1447 (1446 Ra), 1155 (1157 Ra) and to a shoulder in the Raman spectrum at 1194 cm^{-1} , as pre-

dicted by the calculations, while the bands at 928 (929 Ra) and 778 (778 Ra) cm^{-1} are assigned to the corresponding out-the plane deformations. The bands in the Raman spectrum at 260 and 220 cm^{-1} are assigned to the Cl-H stretching modes of the dimer of clonidine hydrochloride (Romano et al. Submitted).

CH₂ modes

The group of the bands between 3043 and 2872 cm^{-1} in both spectra are assigned to the asymmetric and symmetric stretching modes of the four species of clonidine, as indicated in TABLE 3^[5-9,24-30]. Note that the asymmetric stretching modes are calculated

at higher wavenumbers than the symmetric modes and, for this, the symmetric modes can be assigned to the strong bands in IR and Raman spectra at 3007, 2986, and 2960 cm^{-1} , while the asymmetric modes are assigned to the IR and Raman bands of medium intensity at 2950, 2920, 2906 and 2872 cm^{-1} , as can be seen in TABLE 3. The IR bands at 1493, 1485 and 1466 cm^{-1} are clearly assigned to the scissoring modes according to similar compounds containing the CH_2 group^[5-9,24-30] while, the medium IR bands at 1340 and 1294 cm^{-1} are easily assigned to the wagging modes, as predicted by the calculations. The weak IR bands at 1206 and 1198 cm^{-1} are assigned to the expected rocking modes while, in the Raman spectrum these modes appear at 1206 and 1165 cm^{-1} with medium intensity^[5-9,24-30]. The weak band and a shoulder in IR at 1026 and 812 cm^{-1} , respectively and the medium and weak Raman bands at 1028 and 987 cm^{-1} , respectively are associated with the twisting modes.

Skeletal modes

In the clonidine the C=C stretching modes of benzyl ring was assigned to the bands at 1581, 1567, 1264 and 1075 cm^{-1} in IR and to the Raman bands at 1582, 1570, 1542, 1264 and 1071 cm^{-1} . The C-C stretching mode of imidazole ring does not appear in the infrared spectrum, but a weak signal in Raman is observed in accordance to the related compounds^[7,8,22,24-28]. The bands in the infrared spectrum at 421 and 402 cm^{-1} are assigned to the C-Cl stretching modes of clonidine hydrochloride (*Romano et al. Submitted*). The in-plane deformation modes appear in Raman as a strong band at 293 cm^{-1} and a very weak band at 186 cm^{-1} while the out-of-plane deformation modes are predicted at higher wavenumbers, thus, these modes are associated with the bands at 525 and 518 cm^{-1} in the IR spectrum. The bands in the IR spectrum at 1091, 669 and 686 cm^{-1} are associated to the in-plane deformations of the phenyl ring. These modes for the imidazole ring are associated to the bands at 973 and 686 cm^{-1} in the IR, and to the Raman at 973 and 587 cm^{-1} . Moreover, the IR bands at 618 and 535 cm^{-1} and the two weak Raman bands at 1091 and 766 cm^{-1} were assigned to the torsion benzyl rings modes while these modes for the imidazole rings are attributed to the

bands in the Raman spectrum at 169 and 126 cm^{-1} .

FORCE FIELD

The force constants for the three tautomers of clonidine and their protonated form were calculated in gas phase at the B3LYP/6-31G* and B3LYP/6-311++G** levels from the corresponding scaled force fields with the Molvib program^[16] and they were expressed in terms of internal coordinates. These constants were compared in TABLE 4 with those obtained for the anti-hypertensive 2-(2-benzofuranyl)-2-imidazoline^[8] and tolazoline hydrochloride^[9] agents at the same levels of theory. The results show the notable influence of the size of the basis sets on the calculated force constants values. Hence, when the size of the basis set change of 6-31G* at 6-311++G** increase the force constant values. The results for the diverse species of clonidine show that in general the values are slightly higher for the tautomer II, while the protonated species present the highest values with both basis sets than the other ones. In general, the presence of the Cl atoms in the benzyl rings of all the species of clonidine increase the $f(\nu\text{N-C})$ and $f(\nu\text{C-H})_{\text{benc}}$ force constants, in relation to the two anti-hypertensive agents compared. Note that the $f(\nu\text{C-C})_{\text{imid}}$ and $f(\nu\text{C-H})_{\text{imid}}$ force constants of tolazoline hydrochloride^[9] present the highest value in relation to the species of clonidine demonstrating, this way, that the imidazoline rings in all the species are also influenced by the Cl atoms of the benzyl rings. On the other hand, the $f(\nu\text{C-Cl})$ and $f(\nu\text{C-C})_{\text{benc}}$ force constants values increase due to the presence additional of the Cl atoms in the hydrochloride species while decrease the $f(\nu\text{N-H})$ force constant value, as expected because the N-H bond are linked to that additional Cl atom (*Romano et al. Submitted*).

HOMO-LUMO

The frontier orbitals^[5,24] were calculated for the tautomers of clonidine and their protonated form in order to predict their reactivities by using both approximation levels and the values are presented in TABLE S11 compared with those values calculated

ORIGINAL ARTICLE

for clonidine hydrochloride and for tolazoline hydrochloride and their protonated species. The results for all the species show that the frontier orbitals are mainly located in the rings and are antibonding orbital π -type. The greater reactivity in the gas phase is observed for clonidine hydrochloride where the reactivity decrease according the following order: H > CIT > IB > PT > IA > II > P using the 6-31G* basis set while the order change using the 6-311++G** basis set at: H > CIT > IB > IA > PT > II > P. A very important result is the notable increase in the reactivity of clonidine when two Cl atoms are incorporate to the phenyl ring, in relation to tolazoline (see Figure S4). Obviously, the hydrochloride forms are more reactive in both anti-hypertensive agents due to the presence of the Cl atoms but, the additional presence of two Cl atoms in the phenyl ring is essential for increase the reactivity of a hydrochloride species. On the other hand, we observed that the chemical group between the two phenyl and imidazoline rings in an anti-hypertensive agent is a important requirement for their reactivity, thus, the N-H group increase the reactivity of clonidine hydrochloride, as compared with tolazoline hydrochloride where the separation between those pairs of rings are performed by means of the CH₂ group.

CONCLUSIONS

In the present work, we have reported the theoretical molecular structures of the three tautomers of clonidine and their protonated form by using the B3LYP/6-31G* and B3LYP/6-311++G** methods. The Synchronous Transit-Guided Quasi-Newton (STQN) method using was used to study the interconversion between the three tautomers of clonidine and the reaction paths connecting these three structures with the corresponding transition states. The NBO study reveals the high stability of the tautomer II in relation to the other ones while the AIM analysis support the probable presence of the tautomers IA and IB in the solid phase due to the intra-molecular H bonds formation in both species in gas phase. The study of the bond orders for the N atoms of the tautomer II and their protonated species evidence clearly a chemically equivalent environmental due

to that those atoms in the two species are protonated. The analysis of the frontier orbitals for the clonidine and tolazoline hydrochloride species suggest that the presence of two Cl atoms in the phenyl rings is essential for increase the reactivity of a hydrochloride species. Moreover, the chemical group between the two phenyl and imidazoline rings in an anti-hypertensive agent is a important requirement for their reactivity, thus, the N-H group increase the reactivity of clonidine hydrochloride, as compared with tolazoline hydrochloride where the separation between those pairs of rings are performed by means of the CH₂ group. The complete vibrational assignments for the four studied species were performed combining the available infrared and Raman spectra for clonidine hydrochloride with the Scaled Quantum Mechanics Force Field (SQMFF) procedure. In addition, the force constants for the four species of clonidine were reported and compared with those obtained for similar antihypertensive agents.

ACKNOWLEDGEMENTS

This work was subsidized with grants from CIUNT (Consejo de Investigaciones, Universidad Nacional de Tucumán). The authors thank Prof. Tom Sundius for his permission to use Molvib.

REFERENCES

- [1] D.Romani, M.J.Márquez, M.B.Márquez, S.A.Brandán; *J.Mol.Struct.*, **1100**, 279-289 (2015).
- [2] D.Romani, S.A.Brandán; *Comput.Theoret.Chem.(Theochem)*, 10.1016/j.comptc.2015.03.018, **1061**, 89-99 (2015).
- [3] M.J.Márquez, M.B.Márquez, P.G.Cataldo, S.A.Brandán; *OJTA*, **4**, 1-19 (2015).
- [4] Pablo G.Cataldo, María V.Castillo, Silvia A.Brandán; *Phys.Chem.& Biophysics*, **4(1)**, 1-9 (2014).
- [5] M.B.Márquez, S.A.Brandán; *International Journal of Quantum Chemistry*, **114**, 209-221 (2014).
- [6] E.Romano, F.Ladetto, S.A.Brandán; *Computational & Theoretical Chemistry*, **1011**, 57-64 (2013).
- [7] E.Romano, M.V.Castillo, J.Pergomet, J.Zinczuk, S.A.Brandán; *Open Journal of Synthesis Theory and Applications*, **2**, 8-22 (2013).
- [8] C.D.Contreras, M.Montejo, J.J.López González,

- J.Zinczuk, S.A.Brandán; *J.Raman Spect.*, **42**(1), 108-116 (2011).
- [9] C.D.Contreras, A.E.Ledesma, J.Zinczuk, S.A.Brandán; *Spectrochim.Acta Part A*, **79**, 1710-1714 (2011).
- [10] S.Ghose, J.K.Dattagupta; *J.Chem.Soc.Perkin Trans II*, 599-601 (1989).
- [11] Jr.R.R.Ruffolo, W.Bondinell; *J.P.Hieble.J.Med.Chem.*, **38**(19), 3681-3716 (1995).
- [12] C.Farsang, J.Kapocsi; *Brain Res.Bull.*, **49**(5), 317-331 (1999).
- [13] J.Tank, A.Diedrich, E.Szczzech, F.C.Luft, J.Jordan; *Hypertension*, **43**, 1035-1041 (2004).
- [14] M.Remko, M.Swart, F.M.Bickelhaup; *Bioorg.Med.Chem.*, **14**, 1715-1728 (2006).
- a) G.Rauhut, P.Pulay; *J.Phys.Chem.*, **99**, 3093-3099 (1995); b) G.Rauhut, P.Pulay; *J.Phys.Chem.*, **99**, 14572 (1995).
- [15] T.Sundius; *Vib.Spectrosc.*, **29**, 89-95 (2002).
- [16] A.D.Becke; *Phys.Rev.*, **A38**, 3098-3100 (1988).
- [17] C.Lee, W.Yang, R.G.Parr; *Phys.Rev.*, **B37**, 785-789 (1988).
- [18] A.E.Reed, L.A.Curtis, F.Weinhold; *Chem.Rev.*, **88**(6), 899-926 (1988).
- [19] E.D.Glendening, J.K.Badenhop, A.D.Reed, J.E.Carpenter, F.Weinhold, NBO 3.1; Theoretical Chemistry Institute, University of Wisconsin; Madison, WI, (1996).
- [20] R.F.W.Bader; *Atoms in Molecules, A Quantum Theory*, Oxford University Press, Oxford, 1990, ISBN: 0198558651.
- [21] F.Biegler-König, J.Schönbohm, D.Bayles; *J.Comput.Chem.*, **22**, 545 (2001).
- [22] R.G.Parr, R.G.Pearson; *J.Am.Chem.Soc.*, **105**, 7512-7516 (1983).
- [23] D.Romani, S.A.Brandán; *Arabian Journal of Chemistry*, <http://dx.doi.org/10.1016/j.arabjc.2015.06.030>, (2015).
- [24] A.B.Nielsen, A.J.Holder; *Gauss View 3.0, User's Reference*, GAUSSIAN Inc., Pittsburgh, PA, 2000-2003.
- [25] *Gaussian 03, Revision B.01*, M.J.Frisch, G.W.Trucks, H.B.Schlegel, G.E.Scuseria, M.A.Robb, J.R.Cheeseman, J.A.Jr.Montgomery, T.Vreven, K.N.Kudin, J.C.Burant, J.M.Millam, S.S.Iyengar, J.Tomasi, V.Barone, B.Mennucci, M.Cossi, G.Scalmani, N.Regga, G.A.Petersson, H.Nakatsuji, M.Hada, M.Ehara, K.Toyota, R.Fukuda, J.Hasegawa, M.Ishida, T.Nakajima, Y.Honda, O.Kitao, H.Nakai, M.Klene, X.Li, J.E.Knox, H.P.Hratchian, J.B.Cross, C.Adamo, J.Jaramillo, R.Gomperts, R.E.Stratmann, O.Yazyev, A.J.Austin, R.Cammi, C.Pomelli, J.W.Ochterski, P.Y.Ayala, K.Morokuma, G.A.Voth, P.Salvador, J.J.Dannenberg, V.G.Zakrzewski, S.Dapprich, A.D.Daniels, M.C.Strain, O.Farkas, D.K.Malick, A.D.Rabuck, K.Raghavachari, J.B.Foresman, J.V.Ortiz, Q.Cui, A.G.Baboul, S.Clifford, J.Cioslowski, B.B.Stefanov, G.Liu, A.Liashenko, P.Piskorz, I.Komaromi, R.L.Martin, D.J.Fox, T.Keith, M.A.Al-Laham, C.Y.Peng, A.Nanayakkara, M.Challacombe, P.M.W.Gill, B.Johnson, W.Chen, M.W.Wong, C.Gonzalez, J.A.Pople, Gaussian; Inc., Pittsburgh PA, (2003).
- [26] C.Peng, H.B.Schlegel; *Israel J.Chem.*, **33**, 449-454 (1993).
- [27] G.Byre, A.Mostad, C.Roming; *Acta Chem.Scand.B*, **30**, 9 (1976).
- [28] E.Romano, F.Ladetto, S.A.Brandán; *Computational & Theoretical Chemistry*, **1011**, 57-64 (2013).
- [29] K.Guzzetti, A.B.Brizuela, E.Romano, S.A.Brandán; *J.Molec.Struct.*, **1045**, 171-179 (2013).